Supplementary Information

Effect of reduced graphene oxide (rGO) compaction degree and concentration on rGO-polymer composites printability and cell interactions

*María Cámara-Torres [1], Ravi Sinha [1], Siamak Eqtesadi [2], Rune Wendelbo [2], Marco Scatto [3], Paolo Scopece [3], Alberto Sanchez [4], Sara Villanueva [4], Ainhoa Egizabal [4], Noelia Álvarez [4], Alessandro Patelli [5], Carlos Mota [1], Lorenzo Moroni [1]***

[1] Maastricht University, MERLN Institute for Technology-Inspired Regenerative Medicine, Complex Tissue regeneration Department, Universiteitssingel 40, 6229 ER Maastricht, The Netherlands.

[2] Abalonyx AS, Forskningsveien 1, 0373 Oslo, Norway.

[3] Nadir S.r.l., Via Torino, 155/b, 30172 Venice, Italy.

[4] TECNALIA, Basque Research and Technology Alliance (BRTA), Mikeletegi Pasealekua 2, 20009 Donostia-San Sebastian, Spain.

[5] Department of Environmental Sciences, Informatics and Statistics, Ca' Foscari University of Venice, Dorsoduro 3246, 30172 Venice, Italy.

[6] Department of Physics and Astronomy, Padova University, Via Marzolo, 8, 35131 Padova, Italy.

* Email corresponding author: l.moroni@maastrichtuniversity.nl

A

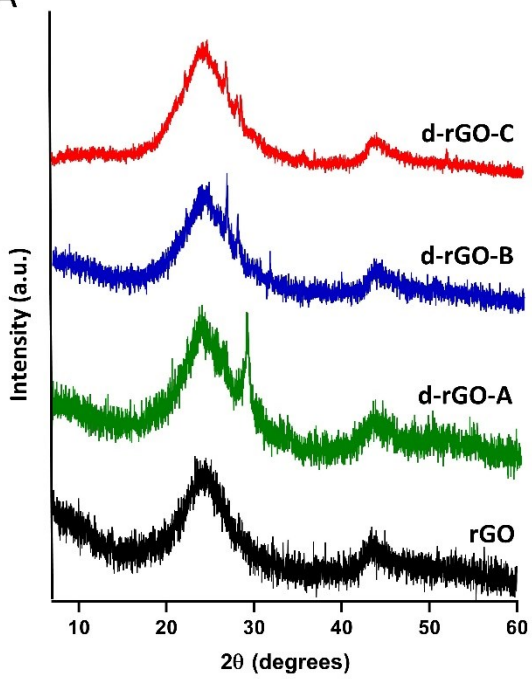

B

Sample	FWHM peak (002) (radians)
rGO	0.12
d-rGO-A	0.14
d-rGO-B	0.11
d-rGO-C	0.13

Figure S1. (A) XRD diffraction patterns of the three different d-rGO used in this study, each coming from different rGO batches. (B) Full width at half maximum (FWHM) of (002) diffraction peaks.

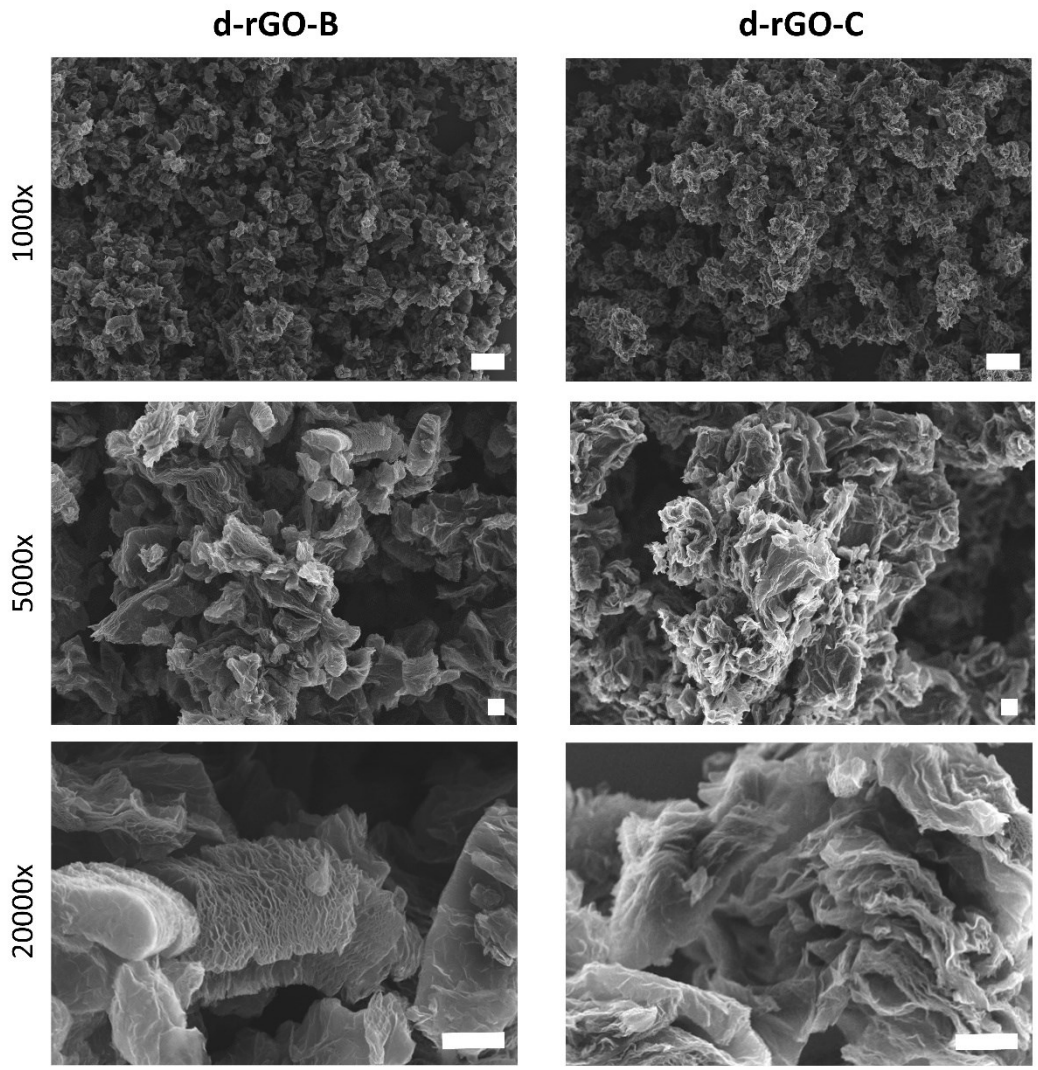

Figure S2. Representative SEM images of d-rGO-B and d-rGO-C at different magnifications, displaying different degrees of compaction. Scale bars 20 μm (top row), and 2 μm (middle and bottom row).

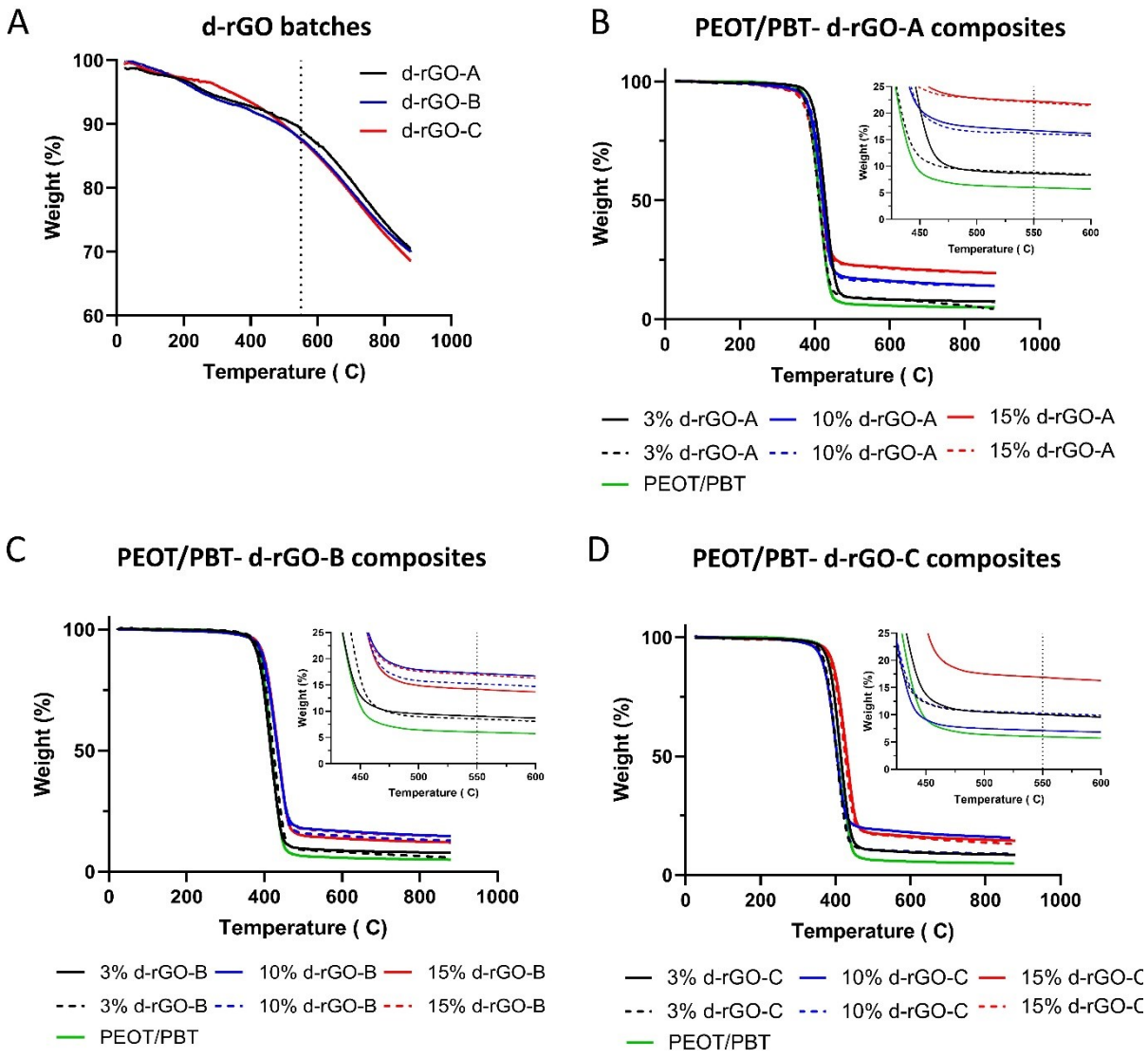

Figure S3. TGA curves of (A) d-rGO batches, (B) PEOT/PBT-d-rGO-A composites, (C) PEOT/PBT-d-rGO-B composites and (D) PEOT/PBT-d-rGO-C composites. For each concentration, two curves, measured from two different samples are represented.

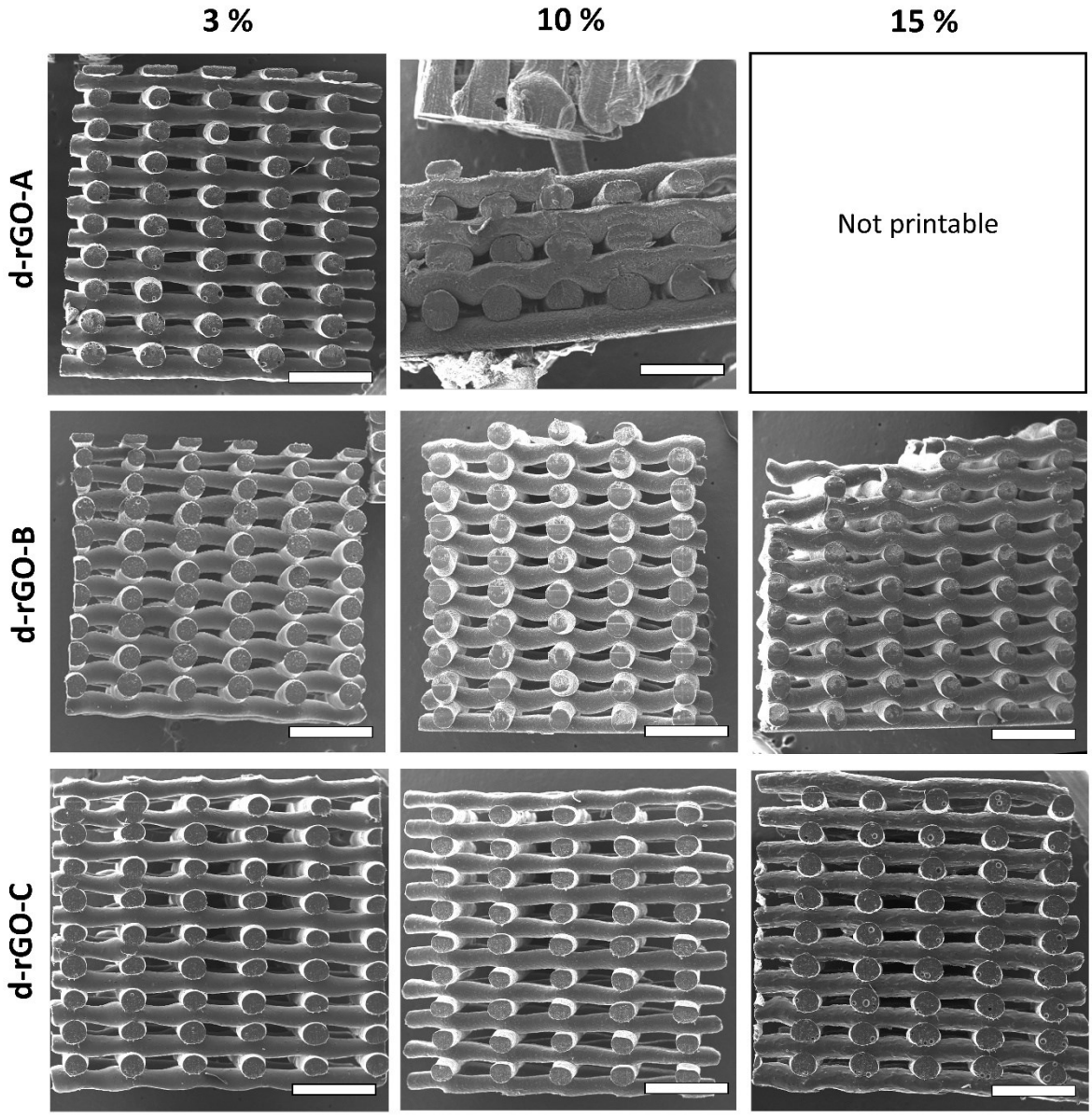

Figure S4. SEM micrographs of 3D ME-AM scaffolds cross sections obtained using each of the d-rGO composites, depicting scaffolds morphology and interconnected porosity. Scale bars 1mm.

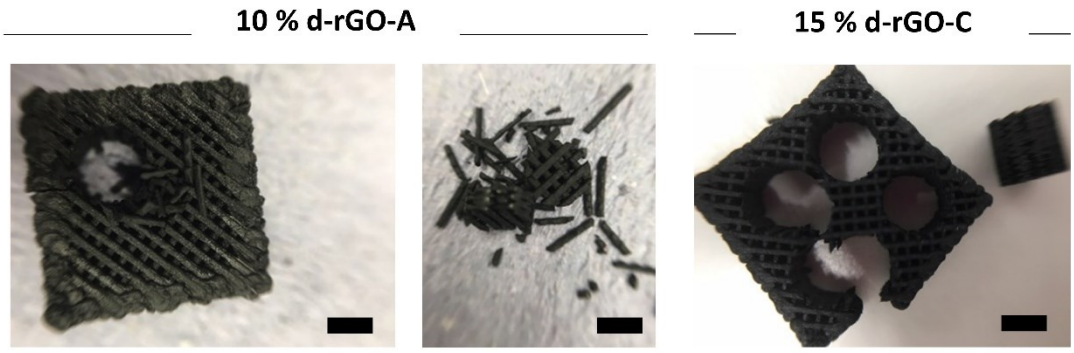

Figure S5 Demonstration of poor layer bonding of 10% d-rGO-A upon punching of scaffold using a biopsy puncher, compared to other scaffold types, such as the 15% d-rGO-C scaffold. Scale bars 2 mm.

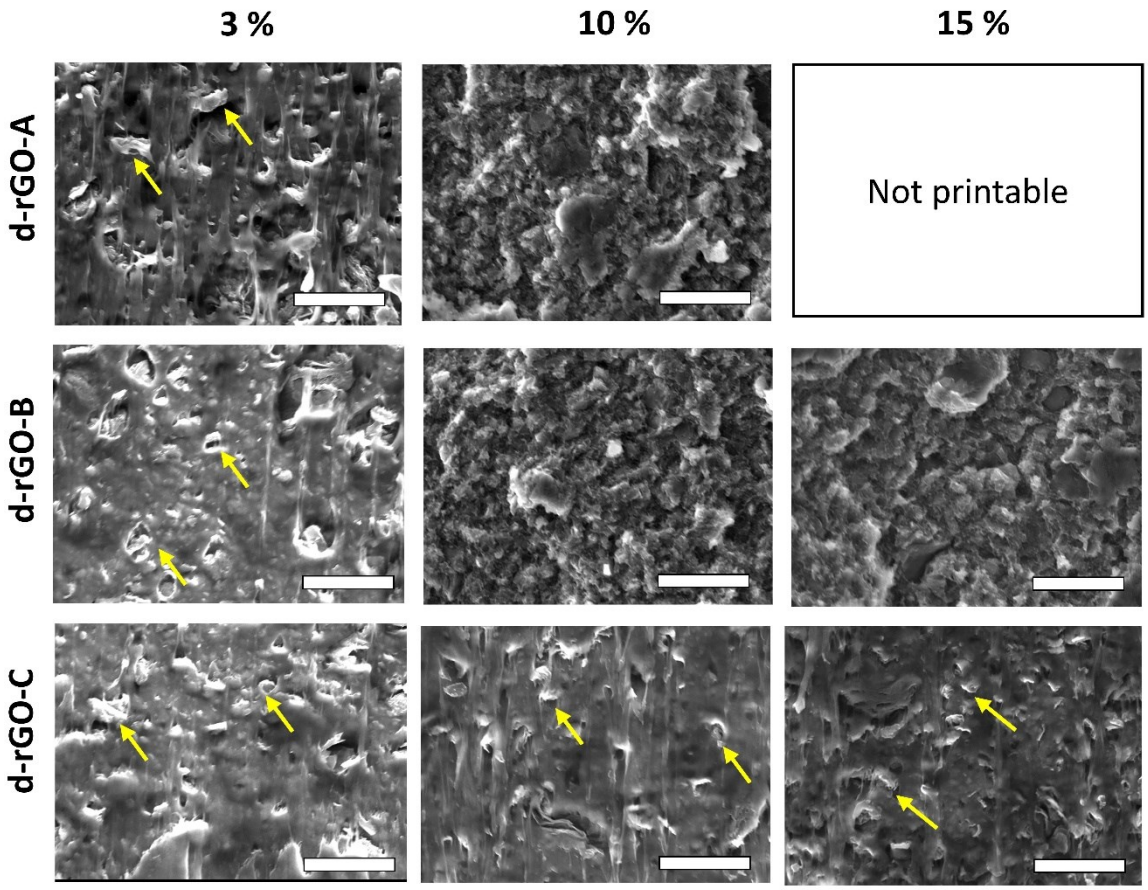

Figure S6. SEM micrographs of 3D ME-AM scaffolds filaments cross sections cut with a razor blade. Yellow arrows indicate rGO particles within the polymer matrix. Scale bars 50 μm.

A

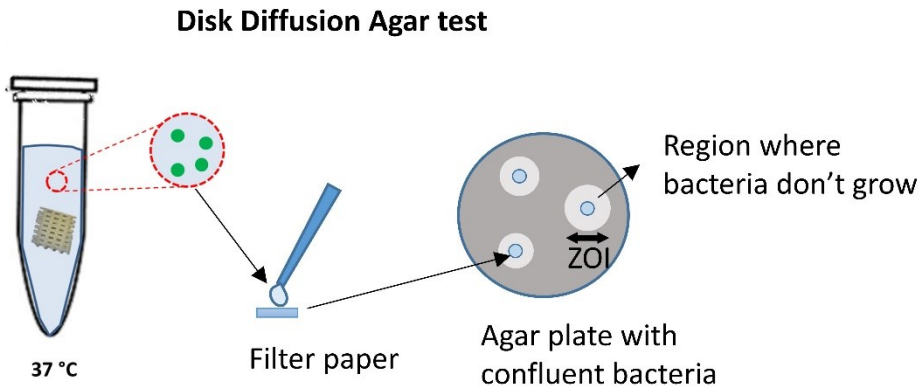

B

	P. aeruginosa (ZOI)			*S. epidermidis* (ZOI)		
	24h	48h	72h	24h	48h	72h
PEOT/PBT	0	0	0	0	0	0
3% d-rGO-B	0	0	0	0	0	0
10% d-rGO-B	0	0	0	0	0	0
15% d-rGO-B	0	0	0	0	0	0

C

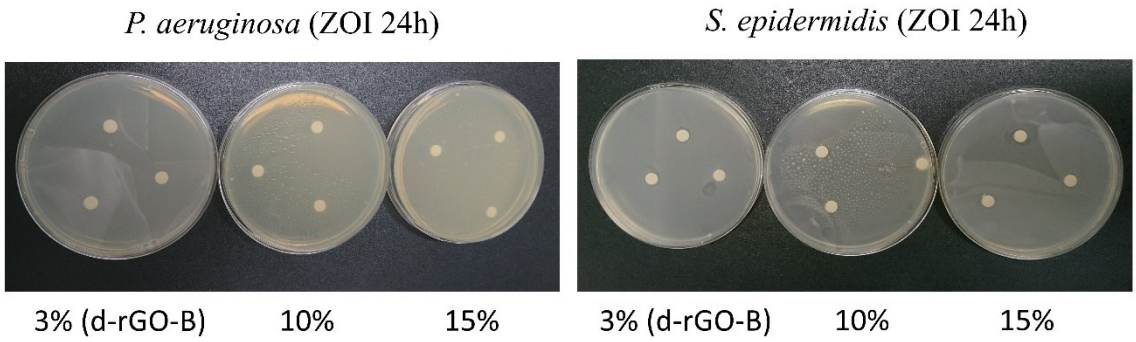

Figure S7. (A) Disk diffusion agar test diagram. (B) Antimicrobial activity of d-rGO-B scaffolds against *P. aeruginosa and S. epidermidis*, measured through the disk diffusion agar test and reported as zone of inhibition (ZOI) values. (C) Images of representative disk diffusion test plates depicting ZOIs around a disk impregnated with an aliquot of the scaffold supernatant after the initial 24h of incubation. Scale bars 5 mm.

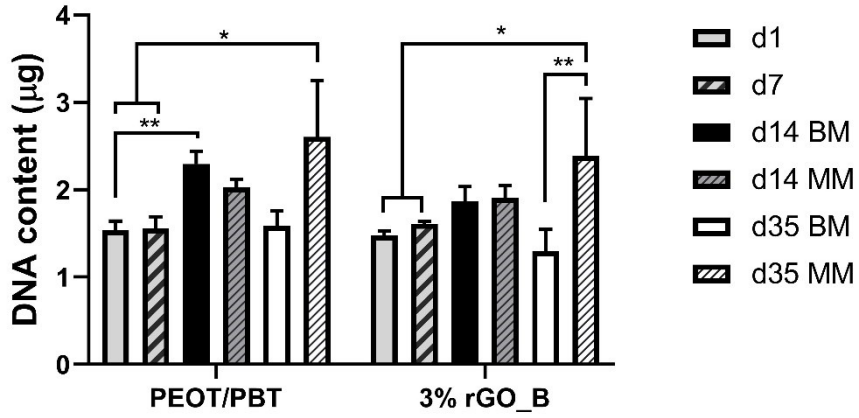

Figure S8. DNA content progression on PEOT/PBT and 3% d-rGO-B scaffolds over 35 days of culture in BM or MM.

Table S1. Atomic compositions (%) of each of the d-rGO measured by XPS.

	C	O	C/O ratio	N	Al	Si	S	Cl	Fe
d-rGO-A	85.3	14.4	5.8	0.0	0.0	0.2	0.0	0.1	0.0
d-rGO-B	83	16	5.2	0.2	0.0	0.6	0.2	0.2	0.0
d-rGO-C	82	16.5	5.0	0.2	0.2	0.6	0.1	0.4	0.1

Table S2. d-rGO-B antimicrobial activity at different concentrations in contact with *P. aeruginosa* and *S. epidermidis*.

Samples	*P. aeruginosa* (R)	*S. epidermidis* (R)
3mg/ml d-rGO-B	> 5.8	> 4.8
10 mg/ml d-rGO-B	> 5.8	> 4.8
15 mg/ml d-rGO-B	> 5.8	> 4.8

Table S3. Antimicrobial activity against P. aeruginosa and S. epidermidis of PEOT/PBT- d-rGO-B films (0.1 g/mL) containing different d-rGO concentrations.

Samples	*P. aeruginosa* (R)	*S. epidermidis* (R)
3% d-rGO-B film	1.3	2.0
10% d-rGO-B film	5.8	4.7
15% d-rGO-B film	6.2	4.7